

Distance Dependence of Electron Transfer Across Peptides with Different Secondary Structures: The Role of Peptide Energetics and Electronic Coupling

Yeung-gyo K. Shin,[§] Marshall D. Newton,^{*,‡} and Stephan S. Isied^{*,†}

Contribution from the Department of Chemistry, Rutgers, the State University of New Jersey, Piscataway, New Jersey 08855, Department of Chemistry, Brookhaven National Laboratory, Upton, New York 11973-5000, and Chemistry and Physics Department, Kean University, Union, New Jersey 07083

Received March 11, 2002; E-mail: isied@rutchem.rutgers.edu

Abstract: The charge-transfer transition energies and the electronic-coupling matrix element, $|H_{DA}|$, for electron transfer from aminopyridine (ap) to the 4-carbonyl-2,2'-bipyridine (cbpy) in cbpy-(gly) $_n$ -ap (gly = glycine, $n = 0-6$) molecules were calculated using the Zerner's INDO/S, together with the Cave and Newton methods. The oligopeptide linkages used were those of the idealized protein secondary structures, the α -helix, 3_{10} -helix, β -strand, and polyproline I- and II-helices. The charge-transfer transition energies are influenced by the magnitude and direction of the dipole generated by the peptide secondary structure. The electronic coupling $|H_{DA}|$ between (cbpy) and (ap) is also dependent on the nature of the secondary structure of the peptide. A plot of $2 \cdot \ln|H_{DA}|$ versus the charge-transfer distance (assumed to be the dipole moment change between the ground state and the charge-transfer states) showed that the polyproline II structure is a more efficient bridge for long-distance electron-transfer reactions ($\beta = 0.7 \text{ \AA}^{-1}$) than the other secondary structures ($\beta \approx 1.3 \text{ \AA}^{-1}$). Similar calculations on charged dipeptide derivatives, $[\text{CH}_3\text{CONHCH}_2\text{CONHCH}_3]^{+/-}$, showed that peptide-peptide interaction is more dependent on conformation in the cationic than in the anionic dipeptides. The α -helix and polyproline II-helix both have large peptide-peptide interactions ($|H_{DA}| > 800 \text{ cm}^{-1}$) which arise from the angular dependence of their π -orbitals. Such an interaction is much weaker than in the β -strand peptides. These combined results were found to be consistent with electron-transfer rates experimentally observed across short peptide bridges in polyproline II ($n = 1-3$). These results can also account for directional electron transfer observed in an α -helical structure (different ET rates versus the direction of the molecular dipole).

Introduction

The role of peptide-bridging groups in long-range electron-transfer (ET) reactions in donor-acceptor complexes and in proteins has been the subject of many theoretical¹⁻¹¹ and experimental¹²⁻¹⁵ investigations. In proteins, ET reactions occur

across multiple peptide chains which separate the donor from the acceptor. Multiple pathways for these reactions have been defined; these include covalently connected atoms, H-bonded atoms, and other nonbonded interactions or combinations thereof.^{12,16-21} Systematic studies of simple and well defined donor-peptide-acceptor molecules have the potential to simplify the analysis of protein ET pathways by separating covalent from H-bonding and medium-mediated pathways. Furthermore, studies of ET reactions across controlled peptide bridges are amenable to theoretical calculation of peptide energetics and electronic coupling. Such studies allow the exploration of different protein conformations and the effects of secondary structure on the rate of ET reactions.

- [†] Rutgers, the State University of New Jersey.
[‡] Brookhaven National Laboratory.
[§] Kean University.
- Ungar, L. W.; Newton, M. D.; Voth, G. A. *J. Phys. Chem. B* **1999**, *103*, 7367-7382.
 - Newton, M. D.; Sutin, N. *Annu. Rev. Phys. Chem.* **1984**, *35*, 437-480.
 - Newton, M. D. *Chem. Rev.* **1991**, *91*, 767-792.
 - Langen, R.; Chang, I.-J.; Germanas, J. P.; Richards, J. H.; Winkler, J. R.; Gray, H. B. *Science* **1995**, *268*, 1733-1735.
 - Bixon, M.; Jortner, J. *J. Chem. Phys.* **1997**, *107*, 5154-5170.
 - Jordan, K. D.; Paddon-Row, M. N. *Chem. Rev.* **1992**, *92*, 395-410.
 - Felts, A. K.; Pollard, T.; Friesner, R. A. *J. Phys. Chem.* **1995**, *99*, 2929-2940.
 - Larsson, S. *Chem. Scr.* **1988**, *28A*, 15-20.
 - Larsson, S. *J. Am. Chem. Soc.* **1981**, *103*, 4034-4040.
 - Larsson, S. *J. Chem. Soc., Faraday Trans.* **1983**, *79*, 1375-1388.
 - Jortner, J.; Bixon, M. In *Electron Transfer-From Isolated Molecules to Biomolecules*; Prigogine, I., Rice, S. A., Eds.; John Wiley & Sons: New York, 1999; Vols. 106 and 107.
 - Isied, S. S.; Ogawa, M. Y.; Wishart, J. F. *Chem. Rev.* **1992**, *92*, 381-394.
 - Ogawa, M. Y.; Wishart, J. F.; Young, Z.; Miller, J. R.; Isied, S. S. *J. Phys. Chem.* **1993**, *97*, 11456-11463.
 - Song, X.; Lei, Y.; Van Wallendael, S.; Perkovic, M. W.; Jackman, D. C.; Endicott, J. F.; Rillema, D. R. *J. Phys. Chem.* **1993**, *97*, 3225-3236.

- Chen, P.; Meyer, T. J. *Chem. Rev.* **1998**, *98*, 1439-1477.
- Langen, R.; Colon, J. L.; Casimiro, D. R.; Karpishin, T. B.; Winkler, J. R.; Gray, H. B. *J. Bioinorg. Chem.* **1996**, *1*, 221-225.
- Winkler, J. R.; Gray, J. B. *J. Biol. Inorg. Chem.* **1997**, *2*, 399-404.
- Moreira, I.; Sun, J.; Cho, M.-o. P.; Wishart, J. F.; Isied, S. S. *J. Am. Chem. Soc.* **1994**, *116*, 8396-8397.
- Sun, J.; Wishart, J. F.; Gardineer, M. B.; Cho, M.-o. P.; Isied, S. S. *Inorg. Chem.* **1995**, *34*, 3301-3309.
- Wishart, J. F.; Sun, J.; Cho, M.-o. P.; Su, C.; Isied, S. S. *J. Phys. Chem. B* **1997**, *101*, 687-693.
- Ogawa, M. Y.; Moreira, I.; Wishart, J. F.; Isied, S. S. *Chem. Phys.* **1993**, *176*, 589-600.

The electronic coupling between adjacent or nearby amide linkages in proteins is also of interest to compare with saturated and unsaturated hydrocarbons.^{22–25} Such comparisons will lead to a better understanding of the nature of the peptide orbitals involved in the ET reactions, thus contributing to the ultimate goal of a more detailed understanding of the rates and mechanisms of ET reactions in proteins.

Important questions concerning the distance dependence of ET rates across bridging peptides arose in studies of the intramolecular reactions for the series of donor–peptide–acceptor molecules with different bridging peptides, [(bpy)₂Ru^{II}-cbpy*–peptide–M(NH₃)₅] and [(bpy)₂Ru^{II}-cbpy*–peptide–apRu^{III}-(NH₃)₅] (cbpy = 4-methyl-4'-carboxy-2,2'-bipyridine; M = Co^{III}, Ru^{III}; ap = 4-aminopyridine)^{12,26} and in a number of other recent studies.^{27–34} In a different study, rates for ET reactions in peptides aligned with or against the direction of the peptide dipole in an α -helix were found to differ.³⁵ Such directional rate differences were not present in polyproline II or other random coil structures³⁶ where only weak dipoles exist.

To explore these issues, we have selected a series of peptide-bridged donor–acceptor molecules, cbpy-(gly)_n-ap, for computational studies using the Mulliken–Hush,^{37,38} Cave–Newton³⁹ methods. These molecules represent the organic fragment of the molecules assembled by Isied and co-workers for the studies of the distance dependence of ET across polypeptides.^{12,26} The bridging peptide was constrained to different protein secondary structures, α -helix, 3₁₀-helix, β -sheets, and polyproline helical structures. The lowest electronic transition energies, ΔE , leading to charge separated states in these molecules were calculated using ZINDO/S method for both the cbpy-to-ap and ap-to-cbpy directions in molecules with different numbers of glycine residues (eqs 1 and 2). The sensitivity of these charge-transfer transition energies to specific secondary structures will be presented, as well as the changes in the electronic coupling matrix elements $|H_{DA}|$ between the donor and the acceptor in peptides with different secondary structures. In a separate calculation, the charge-shift reaction in cationic and anionic dipeptides ([CH₃CONHCH₂CONHCH₃]^{+/-}) was also studied for different peptide secondary structures. The insights from these studies were then used to rationalize the

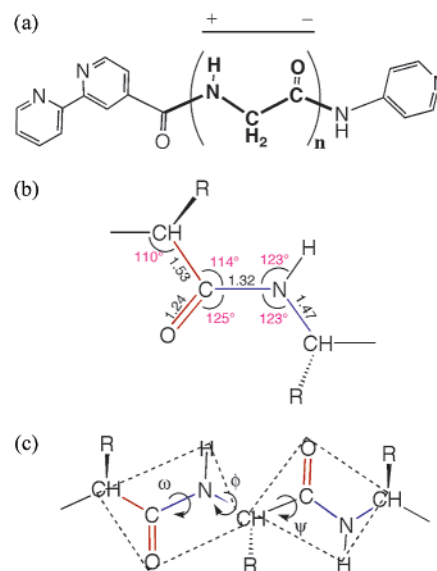
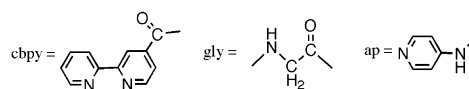
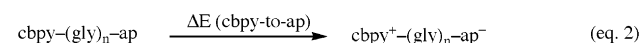
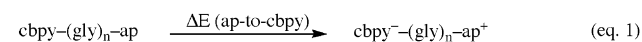


Figure 1. (a) cbpy-(gly)_n-ap, acceptor–peptide–donor molecule with the amino terminal of the first amino acid bound to the carboxy group of the bipyridine acceptor. (b) Structure of a trans peptide residue (taken from ref 41). (c) Peptide conformation showing the ϕ (180°), ψ (180°), and ω (180°) dihedral angles.

Table 1. Dihedral Angles for Peptides with Different Secondary Structures^{34,35}

structure	ω (deg)	ϕ (deg)	ψ (deg)
α -helix	180	-67	-60
polypro II	180	-64	126
3 ₁₀ -helix	180	-43	-24
polypro I	0	-95	160
β -strand	180	-117	113

results of different long-range ET experiments in peptide-bridged donor–acceptor complexes and to extrapolate to more complex protein systems.



Construction of cbpy-(gly)_n-ap Molecules and Computational Parameters. The donor–peptide–acceptor molecules with different number of glycine units were constructed using the average structure of the peptide group with specific dihedral angles corresponding to the different peptide secondary structures (Figure 1, Table 1).^{40,41} The sign convention for the helical axis is shown without reference to the sign of the dipole, because the sign of the dipole is seen to change with the different types of secondary structures (Figure 2). The twist angle between the two pyridine rings for the bpy moiety (6.6°) is taken from the Ru^{II}(bpy)₃ structure.⁴² The connection from the C=O group of the cbpy ring to the N-terminals of the peptide bridge and the twist angle for the ap to the peptide bridge were assumed to

- (22) Kurnikov, I. V.; Beratan, D. N. *J. Chem. Phys.* **1996**, *105*, 9561–9573.
 (23) Onuchic, J. N.; Beratan, D. N. *J. Chem. Phys.* **1990**, *92*, 722–733.
 (24) Liang, C.; Newton, M. D. *J. Phys. Chem.* **1992**, *96*, 2855–2866.
 (25) Liang, C.; Newton, M. D. *J. Phys. Chem.* **1993**, *97*, 3199–3211.
 (26) Mutz, M. W.; Case, M. A.; Wishart, J. F.; Ghadiri, M. R.; McLendon, G. L. *J. Am. Chem. Soc.* **1999**, *121*, 858–859.
 (27) Sisido, M.; Tanaka, R.; Inai, Y.; Imanishi, Y. *J. Am. Chem. Soc.* **1989**, *111*, 6790–6796.
 (28) Sasaki, H.; Makino, M.; Masahiko, S.; Smith, T. A.; Ghiggino, K. P. *J. Phys. Chem. B* **2001**, *105*, 10416–10423.
 (29) Bobrowski, K.; Holcman, J.; Poznanski, J.; Wierchowski, K. L. *Biophys. Chem.* **1997**, *63*, 153–166.
 (30) Bobrowski, K.; Poznanski, J.; Holcman, J.; Wierchowski, K. L. In *Long-Range Electron-Transfer Between Proline-Bridged Aromatic Amino Acids*; Wishart, J. F., Nocera, D. G., Eds.; American Chemical Society: Washington, DC, 1998; Vol. 254.
 (31) Lee, H.; Faraggi, M.; Klapper, M. H. *Biochim. Biophys. Acta* **1992**, *1159*, 286–294.
 (32) Jones, G. I.; Lu, L. N.; Fu, H.; Farahat, C. W.; Oh, C.; Greenfield, S. R.; Gosztola, D. J.; Wasielewski, M. R. *J. Phys. Chem. B* **1999**, *103*, 572–581.
 (33) Anglos, D.; Bindra, V.; Kuki, A. *J. Chem. Soc., Chem. Commun.* **1994**, 213–215.
 (34) Polese, A.; Mondini, S.; Bianco, A.; Toniolo, C.; Scorrano, G.; Guildi, D. M. *J. Am. Chem. Soc.* **1999**, *121*, 3446–3452.
 (35) Galoppini, E.; Fox, M. A. *J. Am. Chem. Soc.* **1996**, *118*, 2299–2300.
 (36) Fox, M. A.; Galoppini, E. *J. Am. Chem. Soc.* **1997**, *119*, 5277–5285.
 (37) Hush, N. S. 1967; Vol. 8, p 391.
 (38) Mulliken, R. S. *J. Am. Chem. Soc.* **1952**, *64*, 811.
 (39) Cave, R. J.; Newton, M. D. *Chem. Phys. Lett.* **1996**, *249*, 15–19.

- (40) Mathews, C. K.; Van Holde, K. E. *Three-Dimensional Structure of Proteins*; The Benjamin/Cummings Publishing Co. Inc.: Redwood City, CA, 1990; Chapter 6, pp 171–179.
 (41) Schulz, G. E.; Schirmer, R. H. *Structural Implications of the Peptide Bond* **1979**, 17–26.
 (42) Harrowfield, J. M.; Sobolev, A. N. *Aust. J. Chem.* **1994**, *47*, 763–767.

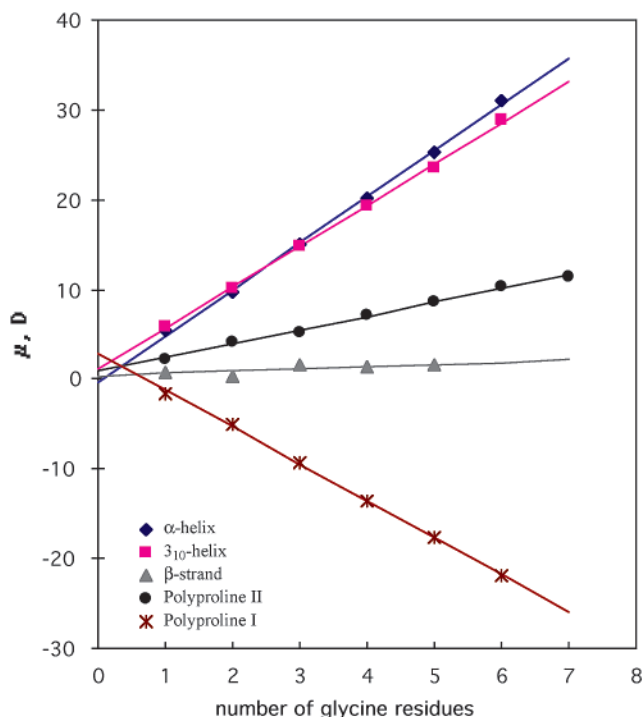


Figure 2. Ground-state molecular dipoles in the direction of helical axes (N-terminal to C-terminal) plotted against the number of gly residues in cbpy-(gly)_n-ap molecules where the (gly)_n residues represent different secondary structural conformations.

Table 2. Orientation of C=O Group with Respect to the Helical Axis and Its Effect on the Molecular Dipole Moment in Different Peptide Secondary Structures

structure	directional cosine ^a	angle (deg)	dipole/residue (D) ^b
α-helix	0.974	13	5.16
polyproline II	0.348	70	1.54
3 ₁₀ -helix	0.886	28	4.57
polyproline I	-0.806	144	-4.10
β-strand	0.215	78	0.25

^a The directional cosine is between the C=O group and the helical axis.

^b Increase in molecular dipole per residue (the slope of the ground-state molecular dipole, μ , vs number of glycine residues shown in Figure 2).

conform to the peptide secondary structure of the bridge under consideration (Table 1).

All semiempirical electronic structure calculations were carried out using the spectroscopic INDO model of Zerner and co-workers (ZINDO/S),⁴³ using the default energy parameters (i.e., scaling parameters $k_{p\sigma} = 1.267$, $k_{p\pi} = 0.585$; resonance integral parameters for O, $\beta(2s) = \beta(2p) = -54.0$ eV). Self-consistent-field (SCF) molecular orbitals (MOs) were obtained at the restricted Hartree–Fock level for the closed-shell ground state in the cbpy-(gly)_n-ap molecule with a SCF tolerance of 0.00001. All the singlet configurations generated by single electron excitations from the highest 30 occupied MOs to the lowest 30 unoccupied MOs were subjected to the CI routine to obtain the spectroscopic quantities used here. The ΔE 's for the lowest-energy charge-transfer (CT) transitions⁴⁴ in both the cbpy-to-ap and ap-to-cbpy directions obtained from these calculations are summarized in Table 2.

(43) Zerner, M. C. *The ZINDO Quantum Chemistry Package*; University of Florida: Gainesville, FL.

(44) The ΔE was plotted against $\Delta\mu_{DA}$ only if the interested transition is found within the lowest 150 transition.

The CT distance, $\Delta\mu_{DA}$, and the corresponding electronic coupling matrix element, $|H_{DA}|$, were determined using eqs 3 and 4. The CT transition studied is that from the ground (diamagnetic) state to the charge-separated (diradical) state in the direction of ap-to-bpy as shown in eq 1. This reaction is related to the oligoproline electron-transfer experiments studied by Isied and co-workers.^{12,21,45} The electronic coupling element, $|H_{DA}|$, between the diabatic ground and charge-separated excited states was calculated using pure adiabatic quantities, i.e., transition energy (ΔE), dipole-moment change upon charge-transfer transition ($\Delta\mu_{12}$), and the transition dipole moment in the direction of $\Delta\mu_{12}$ (μ_{12}).

$$\Delta\mu_{DA} = [(\Delta\mu_{12})^2 + 4(\mu_{12})^2]^{1/2} \quad (3)$$

$$|H_{DA}| = \frac{\mu_{12}\Delta E}{\Delta\mu_{DA}} = \frac{\mu_{12}\Delta E}{[(\Delta\mu_{12})^2 + 4(\mu_{12})^2]^{1/2}} \quad (4)$$

Charge-shift reactions in model $[\text{CH}_3\text{CONHCH}_2\text{CONHCH}_3]^{+/-}$ cationic and anionic dipeptides corresponding to the electron- and hole-transfer superexchange mechanisms³ were separately studied to determine the dependence of $|H_{DA}|$ on peptide conformations and peptide secondary structure (Figure 8).^{6,46,47} The dipeptide structures were taken from the cbpy-(gly)₄-ap structures and the N- and C-terminals were capped with methyl groups to form the dipeptide derivative, $\text{CH}_3\text{CONHCH}_2\text{-CONHCH}_3$.

Results and Discussion

I. Charge-Transfer Energetics and Peptide Secondary Structure. Ground-State Molecular Dipoles and Peptide Secondary Structures. In helical peptides, the ground-state molecular dipole, μ_g , in the direction from the C- to N-terminal axis calculated by the INDO method (Figure 1a) is a linear function of the number of gly residues in the peptide (Figure 2). The magnitude and direction of the molecular dipole in these donor-peptide-acceptor molecules depends on the secondary structure adopted by the peptide (Figure 2). The intercept of Figure 2 corresponds to the ground-state dipole, μ_g , for cbpy-ap (i.e., (2,2'-bipyridine)-CO-NH-(4-aminopyridine)) with the ϕ and ψ dihedral angles for the different peptide secondary structures (Figure 2).⁴⁰ The molecular dipole increment per glycine residue correlates well (Table 2, $R = 0.99$) with the directional cosine for the orientation of the carbonyl groups with respect to the corresponding helical axes. Thus, the molecular dipole for these peptide secondary structures can be approximated as the sum of the local dipoles of the C=O groups of the chain (Figure 3).

For the β -strand and the polyproline II structures (Table 2, Figure 3), only a small increase in the molecular dipole occurs as the number of peptide residues increases. In the polyproline II-helix and the β -strand structures, the molecular dipole increases by 1.5 and 0.25 D per residue, respectively (Table 2, Figure 3). The molecular dipole for the α -helix and the 3₁₀-

(45) Isied, S. S. In *Long-Range Intramolecular Electron-Transfer Reactions Across Simple Organic Bridges, Peptides, and Proteins*; Isied, S. S., Ed.; American Chemical Society: Washington, DC, 1997; Vol. 253, pp 331–347.

(46) Curtiss, L. A.; Naleway, C. A.; Miller, J. R. *Chem. Phys.* **1993**, *176*, 387–405.

(47) Lopez-Castello, J.-M.; Filali-Mouhim, A.; Plante, I. L.; Jay-Gerin, J.-P. *J. Phys. Chem.* **1995**, *99*, 6864–6875.

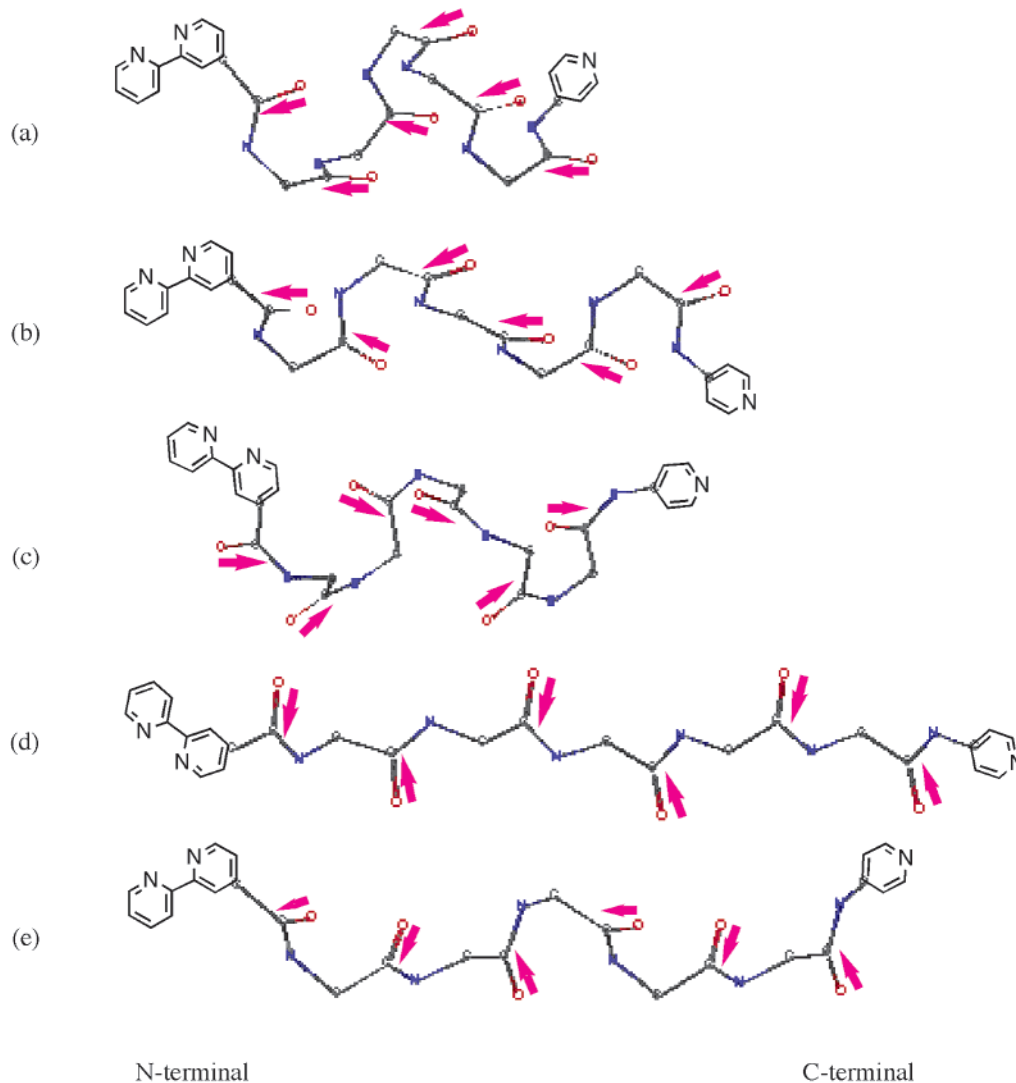


Figure 3. Structures and the local dipole moments for the (gly)₅ residues in the (a) α -helix, (b) 3_{10} -helix, (c) polyproline I-helix, (d) β -strand, and (e) polyproline II-helix conformations. The arrow head represents the positive end of the dipole. The number of carbonyl dipoles used is six, i.e., one more than the number of residue carbonyl groups. The C=O group next to the bipyridine group connects the peptide to the terminal and was included in the electrostatic model.

helix increases by 5.0 and 4.5 D per additional residue, respectively, in the opposite direction of the helical axis (Figure 1a, Table 2, Figure 2). The dipole moment of an isolated peptide unit is estimated to be 3.5 D. If one includes polarization effects due to hydrogen bonding, the dipole moment per residue increases to 5.0 D for the α -helix.^{48,49} In the polyproline I structures, where the peptide bonds are in the cis configuration, their molecular dipoles increase in the direction of the helical axis which is the opposite to that observed in the α -helix and the 3_{10} -helix with an increase of 3.9 D per residue (Figure 2, Table 2).

Charge-Transfer Transition and Dipole Moment Change.

The electronic transitions obtained for the peptide molecules (as described in eqs 1 and 2) are those leading to the lowest-energy charge-separated states. In all molecules studied, a single electronic transition was identified to be associated with the ET excitation, and it corresponds mostly to a single configuration (over >90%). The next lowest transition that takes the

electron from the donor to the acceptor is at least 2000 cm^{-1} higher in energy. The electronic coupling matrix elements ($|H_{DA}|$) were calculated for peptides with different secondary structures from the electronic transition energy between the ground state and the charge-separated state, (ΔE), the associated transition dipole moment, (μ_{12}), and the change in molecular dipole moment between the ground state and the charge-separated state in the direction of charge transfer (eq 4 and Figure 7). The nature of the CT transition was further confirmed by examination of the molecular orbitals involved in the single-electron promoted states that make up the CT configuration. The distance for charge-separation was estimated to be $\Delta\mu_{DA}$ (eq 3).

The interaction between the ground and CT states is expected to be in the nonadiabatic regime, because the transition dipole moment, μ_{12} , is small compared to the change in dipole moment upon charge transfer, $\Delta\mu_{12}$. The difference between $\Delta\mu_{12}$ and $\Delta\mu_{DA}$ is less than 0.1 D (i.e., $\Delta\mu_{DA} \approx \Delta\mu_{12}$); thus, the mixing between the zero-order ground state and charge-separated state is very small. As expected, the CT distances increase as the

(48) Wada, A. *Adv. Biophys.* **1976**, *9*, 1–63.

(49) Hol, W. G. J.; van Duijnen, P. T.; Berendsen, H. J. C. *Nature* **1978**, *273*, 443–446.

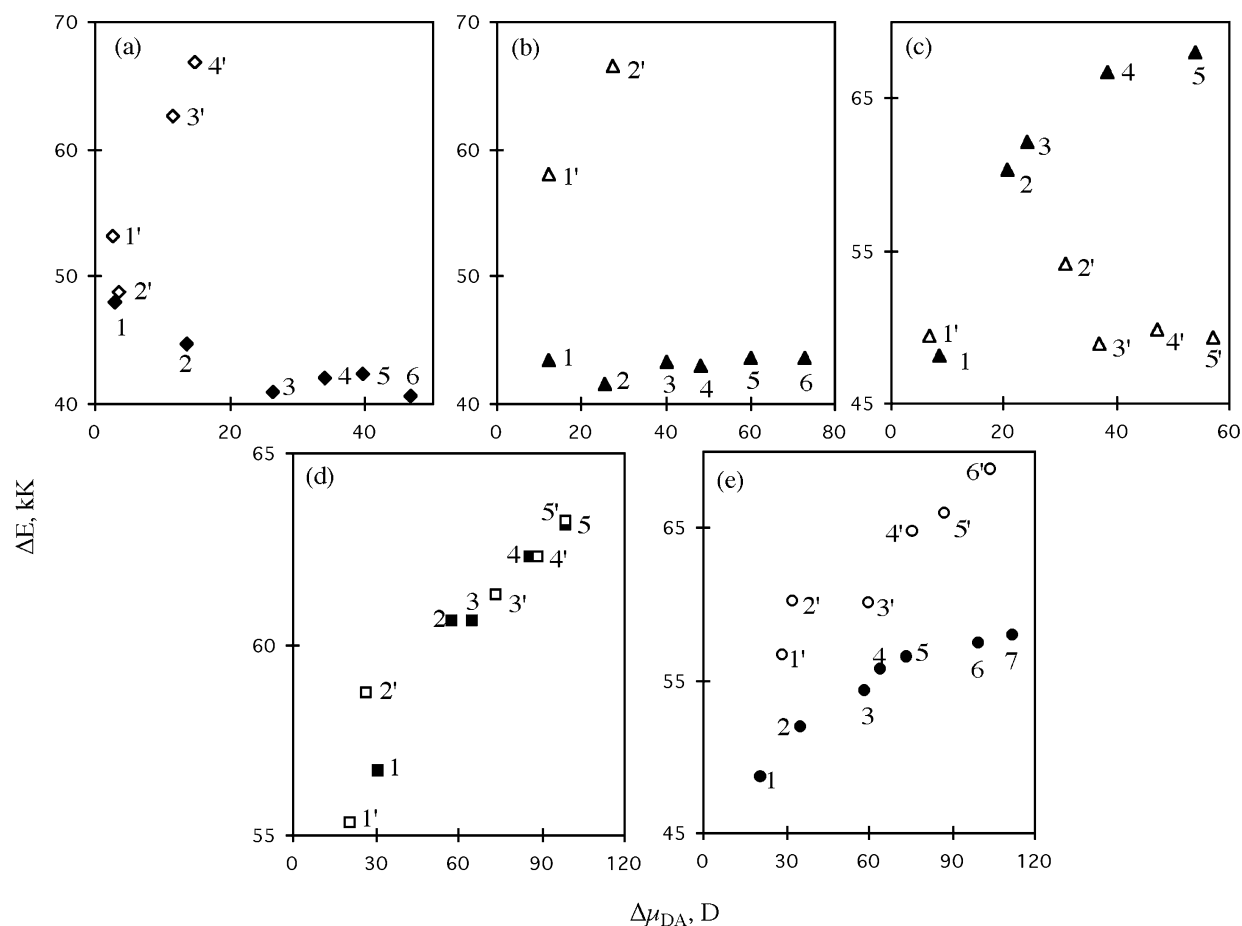


Figure 4. Lowest charge-transfer transition energies plotted against the change in dipole moment in the direction of the ground state molecular dipole for the charge transfer transition in $\text{cbpy}-(\text{gly})_n\text{-ap}$ molecules (complete data for the above plots are presented in Supporting Information). ap-to-cbpy data are also shown in Table 4: (a) α -helix, (b) 3_{10} -helix, (c) polyproline I-helix, (d) β -strand, and (e) polyproline II-helix conformations. Data were collected only when the charge-transfer transition is found within the first 200 CI states. The open legends (with prime notation) are for cbpy-to-ap transitions, and the filled legends are for ap-to-cbpy transitions. Each data point is labeled with the number of gly residues in the peptide bridge.

separation between cbpy and ap groups increases. In small peptides ($n = 1, 2$ residues) where the diameter of the helix is larger than its pitch, the number of gly residues between the donor and the acceptor may not correctly represent the CT distance.

Charge-Transfer Transition Energy: Trends as a Function of Peptide Secondary Structures. The CT transition energy through a peptide depends on the distance of charge separation and the direction of the molecular dipole relative to the direction of the CT. Depending on the bridging peptide secondary structure, two distinct trends are observed for eqs 1 and 2, when their lowest CT energies are plotted vs the dipole moment change, $|\Delta\mu_{\text{DA}}|$ (Figure 4). If the secondary structure of the intervening peptide generates a large molecular dipole, the CT transition energy through such a peptide changes depending on the alignment of the molecular dipole with the direction of the charge transfer. If a molecular dipole for a specific structure is small (e.g., β -strand and polyproline II), the CT transition energy in both directions of eq 1 and 2 increases only slightly as the CT distance increases.

In the α -helix and the 3_{10} -helix, the electric field generated by these molecular dipoles decreases the molecular orbital (MO) energies of cbpy, but increases the MO energies of the ap. The energy required to transfer an electron from the HOMO of ap to the LUMO of cbpy (eq 1) is therefore decreased under the influence of the electric field, while the energy to transfer an

electron from the HOMO of cbpy to the LUMO of ap (eq 2) is increased. Therefore, as the size of the bridging peptide increases,⁵⁰ the transition energy, ΔE , for the cbpy-to-ap transition increases, while ΔE for the ap-to-cbpy transition decreases (Figure 4, a and b).

In the polyproline I structure, the direction of the molecular dipole is opposite to that of the α - and 3_{10} -helices. Thus, the energy needed for transferring an electron in polyproline I shows the reverse trend (Figure 4c) to that observed in the α - and 3_{10} -helices (i.e., the transition energy, ΔE , for the cbpy-to-ap transition slightly decreases, while ΔE for the ap-to-cbpy transition increases as the number of gly residues increases). The smaller molecular dipole generated by the polyproline I structure (as compared to the α -helix or the 3_{10} -helix) results in a smaller ΔE deviations from the pure Coulombic contribution in both CT directions (Figure 4c).

For the β -strand (Figure 4d) and the polyproline II secondary structures (Figure 4e), the peptide dipole has little or no effect on the CT energies, ΔE (see following section). A small increase in ΔE with the number of residues is observed regardless of the direction of the CT transition for both the β -strand and polyproline II structures (for both eqs 1 and 2). Similar results are observed for the hydrocarbon bridges $\text{cbpy}-(\text{CH}_2)_{3n}\text{-ap}$ where

(50) When the D and A groups are placed around the α -helix, the physical separation between D and A does not increase linearly with n .

no molecular dipole formation is possible by the bridging $-(\text{CH}_2)_{3n}-$ group.⁵¹

Factors Governing the Charge-Transfer Transition Energies in Different Peptide Secondary Structures. In calculating the electrostatic potential generated by the Coulombic interaction and the ground-state molecular dipole, the following additional assumptions were also made. (i) The CT transition will transfer one electron. (ii) The distance for charge separation, r_{DA} , is the separation between the carbon atoms that are connected to the peptide-bridge, i.e., 4-C of cbpy and 4-C of ap (Figure 3).

The CT transition energies (eqs 1 and 2) are a function of the charge separation distance as described by the Coulombic interaction between the positive charge on the donor and the negative charge on the acceptor. This Coulombic potential is inversely proportional to the donor–acceptor separation distance; thus, the CT transition energy will increase as this separation distance increases, regardless of the CT direction. In the β -strand or polyproline II structures, where the peptide generates only small ground-state molecular dipoles, the Coulombic contribution is the dominant factor in determining the CT transition energy.⁵² In other secondary structures, the CT transition energy is determined by both the Coulombic potential (of the interaction between the D^+ and A^-) and the local C=O dipoles. The electrostatic potential due to all the carbonyl (peptide bond) dipoles can be calculated by using the point-dipole approximation.⁵³

To assess the effect of local dipoles on the potential of the donor and acceptor, a point dipole of 5 D is placed at the O atom position in the direction of O=C group. The potential due to a point dipole is then calculated to be $|\mu \cdot \mathbf{r}_{\text{a}-\mu(n)}|/|\mathbf{r}_{\text{a}-\mu(n)}|^3$ where μ is the local dipole of the C=O group (5 D), $\mathbf{r}_{\text{a}-\mu(n)}$, $\mathbf{r}_{\text{b}-\mu(n)}$ are distances from ap, cbpy to the n -th dipole, and n is the number of C=O groups used in the structure (i.e. the number of residue C=O's and the cbpy C=O). The potentials at the ap (φ_{a}) and cbpy (φ_{b}), and the transition energy ($\Delta\Delta E$) for charge separation can then be calculated as follows:

$$\text{At 4-C of ap} \quad \varphi_{\text{a}} = \sum_n |\mu \cdot \mathbf{r}_{\text{a}-\mu(n)}|/|\mathbf{r}_{\text{a}-\mu(n)}|^3$$

$$\text{At 4-C of cbpy} \quad \varphi_{\text{b}} = \sum_n |\mu \cdot \mathbf{r}_{\text{b}-\mu(n)}|/|\mathbf{r}_{\text{b}-\mu(n)}|^3$$

$$\text{Transition energy} \quad \Delta\Delta E = \Delta E^\circ + q_{\text{a}}q_{\text{b}}/r_{\text{DA}} + q_{\text{a}}\varphi_{\text{a}} + q_{\text{b}}\varphi_{\text{b}}$$

where r_{DA} is the distance between 4-C of ap and 4-C of cbpy. The effect of the electrostatic interaction is calculated by placing unit charges $q_{\text{a}} = +1$, $q_{\text{b}} = -1$ for the ap-to-cbpy transition, and $q_{\text{a}} = -1$, $q_{\text{b}} = +1$ for cbpy-to-ap transition. To predict the transition energy, the initial energy gap between the donor and

Table 3. Charge-Transfer Transition Energies and Related Parameters for the Electrostatic Model in cbpy-(gly) $_n$ -Ap Molecules in the α -helix and Polyproline II Helix Conformations

no. of gly	d^{a} (Å)	$\varphi_{\text{a}}^{\text{coulomb}}$ (au)	$\varphi_{\text{b}}^{\text{b}}$ (au)	$\varphi_{\text{a}}^{\text{c}}$ (au)	$\Delta\Delta E(\text{ap-cbpy})^{\text{d}}$ (1000 cm^{-1})	$\Delta\Delta E(\text{cbpy-ap})^{\text{e}}$ (1000 cm^{-1})
α -Helix						
1	5.4	0.097	0.052	0.0017	58	55
2	5.0	0.11	0.063	-0.028	47	62
3	6.1	0.087	0.075	-0.076	38	79
4	8.5	0.062	0.082	-0.088	39	89
5	9.9	0.053	0.087	-0.096	38	93
6	10.5	0.050	0.091	-0.10	36	97
7	12.1	0.044	0.094	-0.11	36	100
8	14.0	0.038	0.097	-0.11	36	103
9	15.3	0.034	0.099	-0.12	35	105
10	16.1	0.033	0.10	-0.12	34	106
Polyproline II						
1	6.1	0.087	0.037	-0.012	60	57
2	8.3	0.064	0.042	-0.016	63	64
3	11.5	0.046	0.044	-0.018	66	68
4	14.2	0.037	0.045	-0.020	68	71
5	16.7	0.032	0.046	-0.021	68	73
6	19.7	0.027	0.046	-0.021	69	74
7	22.5	0.024	0.047	-0.022	70	75
8	25.0	0.021	0.047	-0.022	70	76
9	27.8	0.019	0.048	-0.023	70	76
10	30.8	0.017	0.048	-0.023	71	77

^a Distance between the four-carbon atom of cbpy and four-carbon atom of ap. ^b The potential at the four-carbon atom of the cbpy determined by adding the potentials generated by the residue C=O groups and the cbpy C=O. ^c The potential at the four-carbon atom of the ap determined by adding the potentials generated by the residue C=O groups and the cbpy C=O. ^d Energy difference between $\text{cbpy}^- \text{-ap}^+$ and cbpy-ap states. A value of 90 kK was added to $\Delta\Delta E$ to compensate for the energy gap between HOMO of ap and LUMO of cbpy. ^e Energy difference between $\text{cbpy}^+ \text{-ap}^-$ and cbpy-ap states. A value of 65 kK was added to $\Delta\Delta E$ to compensate for the energy gap between HOMO of cbpy and LUMO of ap.

acceptor orbitals (ΔE° , 90 kK to the ap-to-cbpy transition; 65 kK to the cbpy-to-ap transition) was added. Results of these calculations show that, the Coulombic interaction increases the transition energy as the charge-separation distance increases (Table 3), while the contribution of the molecular dipole moment is dependent on the direction of charge transfer vs the direction of the dipole.

For the α -helical structures, the magnitudes of the Coulombic contributions are comparable to the dipole contributions. The CT transition energy is found to increase in the cbpy-to-ap direction as the number of residues increases (eq 1), whereas in the reverse direction, ap-to-cbpy the CT transition is not affected by the change in the number of gly residues. For the polyproline II structure, similar analysis shows that contribution due to peptide dipoles is smaller than that due to Coulombic effects (Table 3, Figure 5). Linear correlation was obtained in the plot of the CT transition energy (ΔE) (obtained from the INDO calculations) with that of the electrostatic energy estimated from the above electrostatic model ($\Delta\Delta E$) (Table 3 and Figure 5).

Since the changes in transition energies associated with the dipole rapidly decrease with increasing distance, the electrostatic field at the termini of a helix should eventually become independent of the length of the helix (experimentally determined for α -helical peptides to be longer than 20 residues).⁵⁴ Therefore, the limiting behavior of the CT transition energy at very long distances for both eqs 1 and 2 is expected to correspond to the Coulombic energy with a constant contribution

(51) A series of $\text{cbpy}-(\text{CH}_2)_{3n}\text{-ap}$ molecules were generated in two different conformations (α - and polyproline II-helices) by replacing the gly residues of the $\text{cbpy}-(\text{gly})_n\text{-ap}$ molecule with $-(\text{CH}_2)_{3n}-$ groups. The C=O and NH groups of donor and acceptor groups were also changed to CH_2 groups. The transition energies for the molecules with $-(\text{CH}_2)_{3n}-$ hydrocarbon bridges were found to be independent of the conformation and direction of charge-transfer (Supporting Information S1). A small increase in ΔE with the number of $-(\text{CH}_2)_{3n}-$ groups was also observed similar to that in the β -strand and polyproline II secondary structures.

(52) Similarly, in hydrocarbon-bridged reference molecules small increases in the transition energies are observed regardless of the direction of CT transition. The slight increase in the CT transition energy with the longer $-(\text{CH}_2)_{3n}-$ bridge can only be due to the Coulombic effects since no carbonyl groups are present in the hydrocarbon bridges to give rise to additional ground-state dipoles.

(53) Jackson, J. D. *Classical Electrodynamics*, 3rd ed.; John Wiley and Sons: New York, 1975; p 138.

(54) Lockhart, D. J.; Kim, P. S. *Science* **1992**, *257*, 947–951.

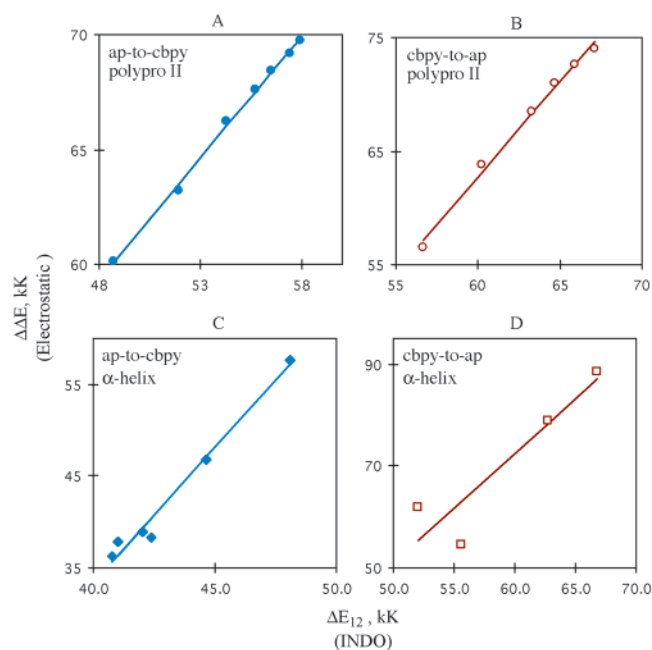


Figure 5. Correlation between the transition energy calculated for the α -helix and polyproline II structures using the INDO and the electrostatic models. A value of 90 kK was added to $\Delta\Delta E$ to compensate for the energy gap between the HOMO of ap and the LUMO of cbpy (A, C). Similarly a value of 65 kK was added to $\Delta\Delta E$ to compensate for the energy gap between the HOMO of cbpy and the LUMO of ap. Note that the transition energies are not only affected by the peptide dipoles but also by the dipoles of the end groups. Since the electrostatic model did not consider the pyridine and the bipyridine dipoles, the difference between the INDO and the electrostatic models becomes noticeable in the first and second points in the “compact” α -helix structure.

from the local dipoles of the intervening peptides. Thus, when the length of the peptide-bridge is more than 20 amino acids, the two transitions (eq 1 and eq 2) should have the same distance dependence, i.e. resulting in two parallel lines as seen in the ΔE vs $\Delta\mu_{DA}$ plot for β -strand in Figure 4d.

II. Electronic Coupling Matrix Element between Peptide Bonds. In this section, calculation of the electronic coupling matrix element, $|H_{DA}|$, of $\text{cbpy}-(\text{gly})_n\text{-ap}$ and its implication for different protein secondary structures will be presented. The $|H_{DA}|$ values were calculated using the spectroscopic parameters obtained from the semiempirical electronic structure calculations.⁴³ Relative electronic coupling for different peptide structures (obtained from the calculation of $|H_{DA}|$) for the molecules in different conformations will also be presented. Finally, ET mechanisms across polypeptides that are consistent with the experimental and theoretical results will be proposed.

Calculation of Electronic Coupling Matrix Elements in Donor–Peptide–acceptor Molecules. The $\text{cbpy}-(\text{gly})_n\text{-ap}$ molecules were constructed to show strong resemblance to the molecules synthesized and studied by Isied, et al.^{12,21,45} in eq 2. In these computational analogues, the two transition metal centers are removed, leaving the organic ligands cbpy and ap as the new donor and acceptor, and the glycine ($-\text{NH}-\text{CHR}-\text{CO}-$; $R = \text{H}$) residue is used in place of the proline peptide for simplicity. Elimination of the transition metal centers reduces the number of orbitals used in the calculations and eliminates uncertainties in the parameters of the second-row transition metal ions.⁵⁵ Replacement of proline with glycine also allows the variation of the peptide conformation using different dihedral angles, ϕ and ψ , corresponding to the different protein secondary

Table 4. Electronic Coupling Matrix Elements and Other Electronic Structure Parameters Obtained for ap to cbpy Charge-Transfer Transition in $\text{cbpy}-(\text{gly})_n\text{-ap}$ Where $(\text{gly})_n$ Units Are in Different Protein Secondary Structural Conformations

n	ΔE (kK)	$ \Delta\mu_{12} $ (D) ^b	$ \mu_{12} $ (D)	$ H_{DA} $ (cm ⁻¹)
α-Helix				
1	48.5	15.5	0.669	2040
2	44.7	17.6	0.570	1450
3	41.0	26.9	0.204	310
4	42.0	37.9	0.446	494
5	42.4	46.2	0.209	191
6	43.7	48.0	0.087	79.0
Polyproline II				
1	48.5	17.8	0.845	2291
2	51.7	38.6	0.357	478
3	54.2	42.1	0.347	447
4	55.7	66.5	0.053	44
5	56.3	82.5	0.103	70.4
6	57.4	99.8	0.0073	3.5
7	57.9	112.5	0.0016	0.82
3_{10}-Helix				
1	43.4	18.2	1.481	3481
2	41.6	29.7	0.121	169
3	43.3	42.9	0.089	90
4	43.0	51.1	0.106	89
5	43.6	62.3	0.009	6.3
6	43.6	74.6	0.002	1.2
Polyproline I				
1	48.2	12.8	1.035	3843
2	60.3	21.8	0.156	431
3	62.1	26.1	0.002	4.8
4	66.7	40.6	0.026	43 ^c
5	68.0	54.5	0.028	37 ^c
β-Sheet				
1	53.6	28.4	0.401	756
2	58.3	38.7	0.118	176
3	60.6	64.3	0.028	25.0
4	62.3	86.1	0.0001	0.11
5	63.1	98.6	0.00005	0.03

^a The analysis employs a two-state model based on the two lowest CI (configuration interaction) states dominated by the local D and A orbitals of the ap and cbpy groups, respectively. In each case, the pair of relevant CI states for the ground state and one excited state (the ordinal label, defined by energy ordering) ranging from number 14–20 (α -helix and 3_{10} -helix) to 18–50 (polyproline II), 29–87 (β -strand), and 17–193 (polyproline I). ^b The corresponding diabatic dipole moment shifts ($\Delta\mu_{DA}$) are calculated to be within 0.1% of the corresponding adiabatic values ($\Delta\mu_{12}$). ^c The calculated $|H_{DA}|$ for this structure is based on high CI states (164 and 193) where the Mulliken–Hush approach may not be applicable.

structures,^{40,41,56,57} namely α -, 3_{10} -, polyproline I- and II-helices, and β -strand.

Electronic coupling matrix elements were calculated only for the charge separation step given in eq 1. The calculated $|H_{DA}|$ (Table 4) are plotted as $2 \cdot \ln(|H_{DA}|)$ vs the change in dipole moment ($\Delta\mu_{DA}$) between the ground state and the charge-separated state (Figure 6). The distance of charge transfer for

(55) In addition to those for the cbpy -peptide- ap molecules, we carried out calculations on the metallo-substituted cpy -peptide molecules ($n = 1, 2, 3$; polyproline) reported in refs 12, 21. The computational method for these calculations was described in ref 58. The result showed similar trends in electronic coupling decays with the charge-transfer distance ($\beta \approx 0.7 \text{ \AA}^{-1}$). This is expected because of the small perturbation introduced by the metal ions. However, it should be mentioned that if the orbital energies of donor and acceptor are in the proximity of the peptide π - and π^* -orbitals, β -values will change. Such systems are not the subject of this work. Effect of specific hydration on β -values was carried out using the method described in ref 58 where specific water molecules around metal ions were introduced. The results here again show no significant change on the β -values. More extensive calculations involving solvents as a continuum are underway and may lead to a further refinement of these conclusions.

(56) Traub, W.; Shmueli, U. *Nature* **1963**, *195*, 1165–1166.

(57) Burge, R. E.; Harrison, P. M.; McGavin, S. *Acta Crystallogr.* **1962**, *15*, 914–915.

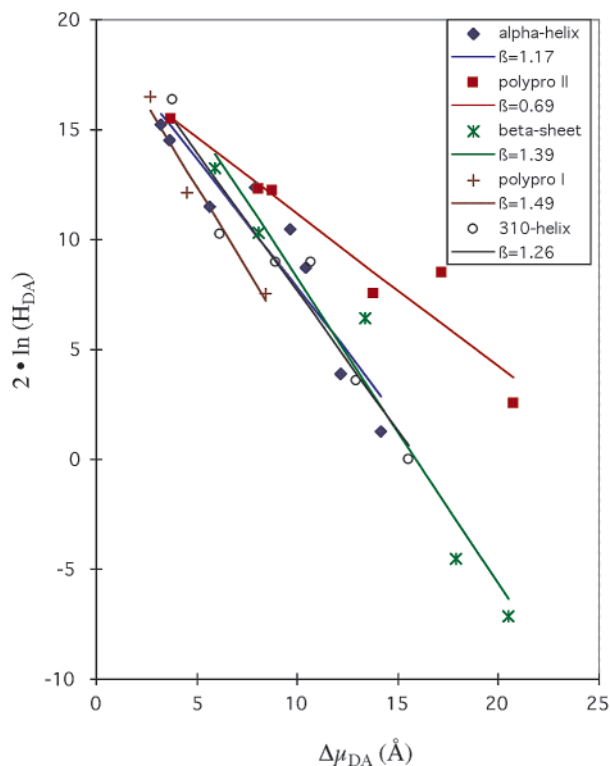


Figure 6. Electronic coupling matrix element ($2 \cdot \ln |H_{DA}|$) plotted against the dipole moment change for the charge transfer transition ($\Delta\mu_{DA}$) in the helical direction in cbpy-(gly) $_n$ -ap molecules with different peptide secondary structures (data taken from Table 4).

the electronic transition is represented by the $\Delta\mu_{DA}$ rather than an arbitrarily chosen physical distance of separation, r_{DA} . This plot allows the direct comparison of the relative electronic coupling in ET reactions for a series of peptides with different secondary structures.

When the bridging (gly) $_n$ groups in cbpy-(gly) $_n$ -ap are in the polyproline II secondary structure, the distance dependence parameter, β (negative slope for the plot of $2 \cdot \ln |H_{DA}|$ vs $\Delta\mu_{DA}$, Figure 6), was calculated to be 0.69 \AA^{-1} . For all the other secondary structures studied, the calculated β values are about twice that obtained in the polyproline II structure (α -helix, 1.17 \AA^{-1} ; β -strand, 1.39 \AA^{-1} ; 3_{10} -helix, 1.26 \AA^{-1} ; polyproline I, 1.49 \AA^{-1}). This result clearly distinguishes the polyproline II structure from the other secondary structures as one with lower distance dependence for ET coupling (Figures 6 and 7). Results of these calculations for $n = 5$ peptide units are shown along with their representative structures as one example for this comparison (Figure 7). Similar calculations using [cbpy * -(proline) $_n$ -apRu $^{III}(\text{NH}_3)_5$] (for $n = 0, 1, 2$) show no significant differences in β -values ($\sim 0.7 \text{ \AA}^{-1}$) than the cbpy-(gly) $_n$ -ap which leads us to conclude that the β -values obtained here are not system specific.^{55,58}

Dipeptide Cationic and Anionic Orbitals. Using the superexchange formalism for ET,^{59–61} electronic coupling in donor-(gly) $_n$ -acceptor complexes, $|H_{DA}|$, can be separated into three different components: donor-gly ($|H_{DB}|$), gly-gly ($|H_{BB}|$), and gly-acceptor ($|H_{BA}|$). In this section, we only

consider the gly-gly electronic coupling ($|H_{BB}|$) in cationic and anionic charge-shift reactions involving the dipeptide model, $[\text{CH}_3\text{CONHCH}_2\text{CONHCH}_3]^{+/-}$, in different secondary structures. These cationic and anionic dipeptides are used as models for hole-transfer and electron-transfer mechanisms, respectively.^{46,47} A schematic energy level diagram for these two cases is given in Figure 8.

The electronic coupling matrix element ($|H_{BB}|$) was determined for the electronic transition responsible for transferring an electron from one peptide π -orbital to the adjacent peptide in the cationic dipeptide. Similar calculations using the π^* -orbitals were carried out for the anionic dipeptide. Only one orbital per bridge site is used in the superexchange model. This is valid because the orbitals responsible for the lowest-energy ET transition are well separated from the next-higher energy orbitals. The orbitals that were used to calculate the $|H_{DA}|$ of cationic dipeptides are those presented in Figure 9. The results of these calculations showed that the $|H_{BB}|$ values for the anionic dipeptides vary only slightly with peptide secondary structure, while $|H_{BB}|$ values for the cationic dipeptides are substantially more sensitive to peptide secondary structure. Recent reports have emphasized the effect of protein thermal nuclear motions on electronic coupling matrix elements^{62–65} and that single $|H_{DA}|$ values for one structure could lead to erroneous conclusions. Since our $|H_{BB}|$ values refer to single structures, we addressed this point by making modest changes in both ϕ and ψ dihedral angles ($\pm 5^\circ$) around the conformations of the stable secondary structures in both the cationic and anionic α -helical dipeptides and recalculated $|H_{DA}|$ for these different conformations. The results show only minor changes in $|H_{DA}|$ values ($\pm 10\%$) occur within a small structural change.

Since the rate constant for ET depends on the square of $|H_{DA}|$, these charge shift reactions would be significantly more sensitive to peptide secondary structure in a hole-transfer rather than an electron-transfer mechanism (Table 5). Thus, experiments for probing the effect of peptide secondary structure are most suitable with donors and acceptors undergoing hole-transfer mechanisms.

Electronic Coupling between Next-Neighbor Peptide Units.

The interaction between two adjacent peptides can occur through the σ -bonding framework of adjacent atoms, or through the π -MOs between two nearest neighboring peptides (i.e., bypassing the connecting -CHR- group). The contour diagram for two HOMO π -orbitals for the cationic dipeptides shows that the interaction between peptide π -orbitals depends on the secondary structure (Figure 9). Partial double bond character of the C-N was proposed earlier by Pauling from work on peptide and protein crystal structures.⁶⁶ The peptide bond can be therefore described as a 3-centered-4-electron bond.^{67,68} The $|H_{DA}|$ for these dipeptides would be sensitive to the π -interaction controlled by the ϕ and ψ dihedral angles between the peptide

(58) Shin, Y.-g. K.; Brunschwig, B. S.; Creutz, C.; Newton, M.; Sutin, N. *J. Phys. Chem.* **1996**, *100*, 1104–1110.

(59) Sutin, N. In *Nuclear and Electronic Factors in Electron Transfer: Distance Dependence of Electron-Transfer Rates*; Bolton, J. R., Mataga, N., McLendon, G., Eds.; American Chemical Society: Washington, DC, 1991; Vol. 228, pp 25–43.

(60) Creutz, C.; Newton, M. D.; Sutin, N. *J. Photochem. Photobiol., A* **1994**, *82*, 47–59.

(61) McConnell, H. M. *J. Chem. Phys.* **1961**, *35*, 508.

(62) Kawatsu, T.; Kakitani, T.; Yamato, T. *J. Phys. Chem. B* **2002**, *106*, 11356–11366.

(63) Balabin, I. A.; Onuchic, J. N. *Science* **2000**, *290*, 114.

(64) Wolfgang, J.; Risser, S. M. *J. Phys. Chem. B* **1997**, *101*, 2986–2991.

(65) Balabin, I. A.; Onuchic, J. N. *J. Phys. Chem.* **1996**, *100*, 11573–11580.

(66) Pauling, L. *The Nature of the Chemical Bond and the Structure of Molecules and Crystals: An Introduction to Modern Structural Chemistry*, 3rd ed; Cornell University Press: Ithaca, NY, 1960.

(67) Wiberg, K. B.; Laidig, K. E. *J. Am. Chem. Soc.* **1987**, *109*, 5935–5943.

(68) Wiberg, K. B.; Breneman, C. M. *J. Am. Chem. Soc.* **1992**, *114*, 831–840.

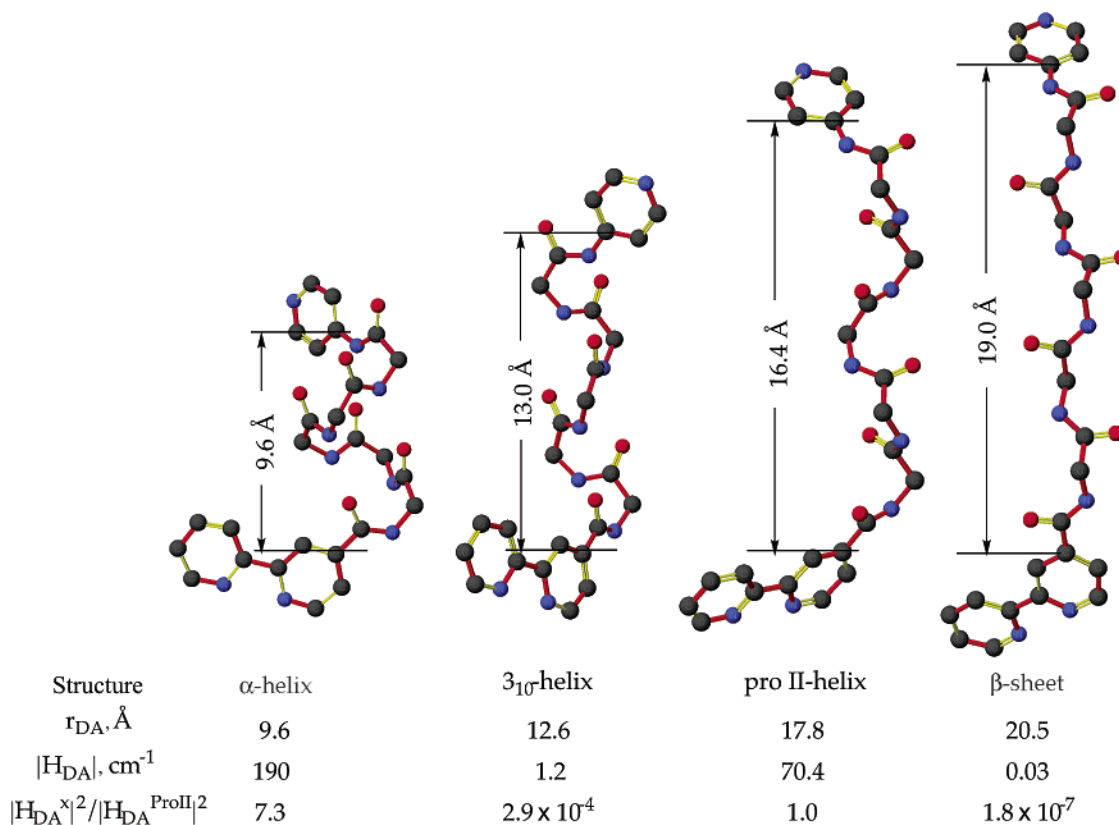


Figure 7. Comparison of the spatial donor–acceptor separation in cbpy-(gly)₅-ap peptides resulting from different secondary-structure conformations. The change in dipole moment (r_{DA}) and the corresponding calculated electronic coupling matrix elements $|H_{DA}|$ are also tabulated. The $|H_{DA}^x|^2/|H_{DA}^{\text{proII}}|^2$ ratios gives a relative ordering of electronic prefactors for all the secondary structures ($n = 5$) compared to the polyproline II structure.

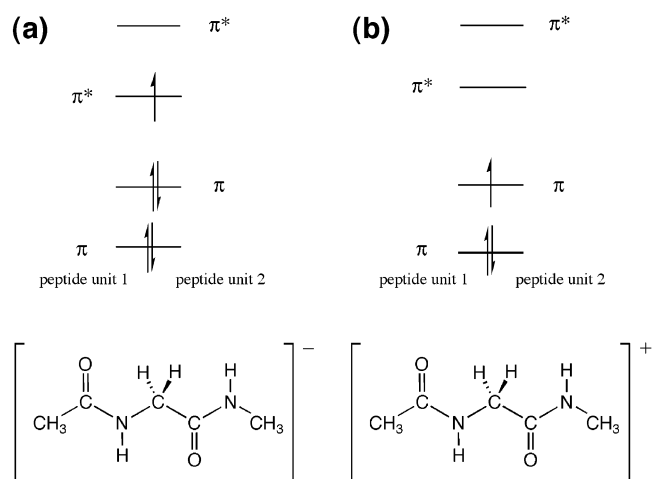


Figure 8. Schematic molecular orbital diagrams for the charge-shift reactions in (a) anionic (electron transfer) and (b) (hole transfer) dipeptides.

residues. Thus the ϕ and ψ dihedral angles which control the orientation between two adjacent peptide residues in different secondary structures can control the electronic coupling between neighboring peptides.

III. Comparison of Theory with Experiments. This theoretical work was initiated to better understand the experimental results of ET across oligoproline residues $n = 1-9$. In the reactions carried out, a large decrease of rate with distance was observed for the first three proline residues followed by a modest decrease for the longer ones beginning from $n = 3$ and continued up to $n = 9$. Other studies also reported this small distance dependence for oligoproline ET.^{12,21,45}

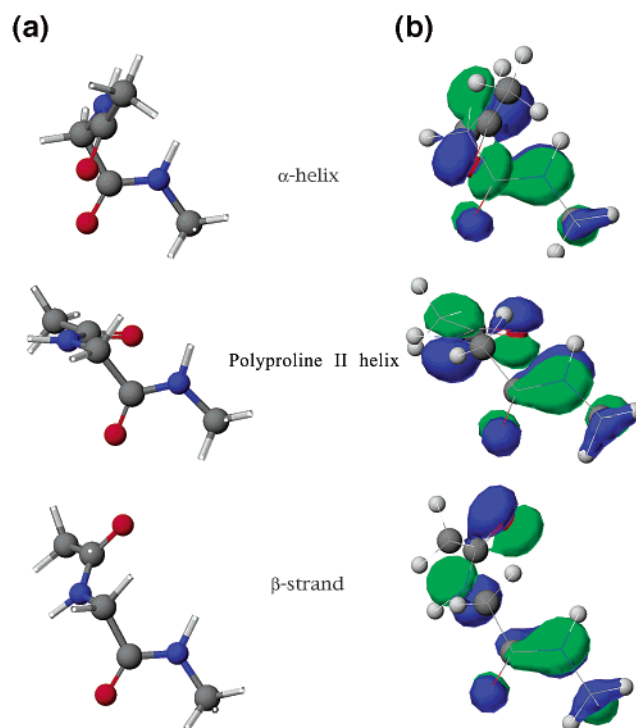


Figure 9. (a) Dipeptide structures and (b) contour diagrams of the highest-occupied MO in each of the radical cations reflecting the interaction between the localized π -orbitals of the two adjacent peptide residues. The polyproline II peptide–peptide interaction is intermediate between the strong interaction in the α -helix and the weaker interaction in the β -strand (Table 5).

For $n = 1-3$ prolines, agreement in the rate vs distance plots for theory and experiment were obtained, where the structures

Table 5. Electronic Coupling Matrix Element for π -Orbitals in Adjacent Dipeptide Derivatives^a

structure	ΔE (kK)	$ \Delta\mu_{12} $ (D) ^b	$ \mu_{12} $ (D)	$ H_{DA} $ (cm ⁻¹)
Monoanionic Dipeptides ^c				
α -helix	10.9	12.7	0.928	777
β -strand	8.9	15.4	1.528	853
polypro II	9.8	12.3	1.004	769
3_{10} -helix	12.7	12.2	0.219	185
Monocationic Dipeptides ^d				
α -helix	17.2	11.6	0.936	1324
β -strand	16.5	18.4	0.157	50
polypro II	16.7	12.2	0.668	870
3_{10} -helix	11.0	7.6	0.550	391

^a Two-state analysis based on the pair of CI states dominated by the local π^* (monoanion) or π (monocation) orbitals of the two peptide residues.

^b Corresponding diabatic dipole moment shifts ($\Delta\mu_{DA}$) are calculated to be within 0.1% of the corresponding adiabatic values ($\Delta\mu_{12}$). ^c For the CI state dominated by 1-electron transition from the MO 27 (HOMO) to MO 28.

^d For the CI state dominated by 1-electron transition from MO 24 to MO 26 (LUMO).

of these short peptide complexes in solution correspond to the polyproline II structure.⁶⁹ An example for such agreement is in the series $(\text{NH}_3)_5\text{Os}^{\text{II}}\text{-Isn-(Pro)}_n\text{-Ru}^{\text{III}}(\text{NH}_3)_5]$ $n = 1-3$; Isn = isonicotinyl group, β (experimental) = 0.68 \AA^{-1} after corrections were made for the distance dependence of reorganization energy⁷⁰ in agreement with the charge-transfer analysis provided here (β (theoretical) = 0.69 \AA^{-1}).

To account for the results of the longer peptides, $n > 4$, one has to consider other mechanisms such as electron- and hole-hopping mechanisms.^{7,11,71,72} For such an ET mechanism, the rate-limiting step is ET from the reduced bpy to the first empty peptide π^* residue, (injection into the peptide bridge) followed by rapid ET between adjacent peptide anions, and finally a rapid peptide to acceptor exothermic step. The computed electronic couplings (H_{DA}) for adjacent peptide-peptide couplings in cationic and anionic peptides are large enough to support rapid multistep reactions at long distances.

In a recent experiment reported using an α -helical structure,^{35,36,73} the influence of the ground state on the molecular dipole in the direction of the ET process was reported. When the ET direction is aligned with the field to generate a molecular dipole, the observed rates were 5 to 27 times faster, depending on the solvent, than the ET rate for the direction against the molecular dipole. No directional dependence of ET rates was observed across the polyproline II structure,^{35,36} in agreement with the small dipole generated by the polyproline II structure and the analysis reported above. Using the simple electrostatic model, the ratio of the ET rates in the direction of the dipole vs against the dipole are calculated to be $8.5^{74,75}$ for the α -helix and only 1.1 for the polyproline II structure, both estimated in an acetonitrile solution ($\epsilon \approx 39$).⁷⁶ The reported experimental ET rate ratios for the α -helix and polyproline II-helices are 7 to 1, respectively. Solvation of these peptide-donor-acceptor molecules would be expected to dampen the effects of the molecular dipoles by the association of solvent molecules with

local dipoles of the individual peptide residues. This solvation effect becomes very important when the CT reaction is between the surface (solvent accessible) and protein interior (solvent inaccessible). In such cases, the structure and solvent effects of the peptide bridge as well as the direction of the CT process need to be considered.

Comparison of the Present Model with Other Theoretical Models for Long-Range ET Reactions. A general theory for estimating the rate of ET reaction assisted by protein matrices has been proposed by Beratan and Onuchic.⁷⁷⁻⁷⁹ The suggested coupling decay of 0.6 for a σ -bond corresponds to an exponential decay constant β of 1.0 per bond. This theory was used to successfully interpret the distance dependence of ET rates between the heme center of cytochrome *c* and ruthenium-modified surface histidine sites.^{17,80} A β -value ranging from 1.1 to 1.4 \AA^{-1} was used to describe the distance dependence of the ET rates in these $\text{Ru}^{\text{II}}(\text{bpy})_2$ -modified proteins.^{4,16,81-83} Furthermore, it was suggested that the decay constant β is smaller for a β -sheet than for an α -helix.^{4,16,17,82} This conclusion is primarily based on the fact that the β -strand covers more through-space distance per peptide residue than does the α -helix (Figures 3, 7). The results obtained in our study for the β -strand and α -helix show similar β -values. In the α -helix, the strong interaction existing between two adjacent peptides results in a small through-space distance (Figure 7), while in the β -strand, the peptide structure is more extended, with fewer peptide residues covering larger distances. The overall similar distance dependence of ET for both secondary structures is a result of the small distance covered with strong interaction (α -helix) as compared to the weaker interaction in the more extended structure (β -strand). The H_{DA} for the α -helix and a β -strand structures in the dipeptide radical cation (Table 5) shows a large difference in magnitude. Future calculations using additional hydrogen-bonding interactions to form a β -sheet (from two β -strands) may provide more insight into other differences in electronic structures between these two secondary structures.

General agreement is observed between the calculations presented here and those of the Beratan-Onuchic theory.^{22,84} The results presented here are complimentary to that of Kurnikov and Beratan who employed σ -type donor and acceptor orbitals to describe the interaction through the peptide backbone. In this work, the nonbonded interactions occurring in peptide

(75) The driving force for the reaction is reported to be $\sim 0.4 \text{ V}$, and the reorganization energy is also reported as $\sim 1.2 \text{ V}$ (using the two-sphere model). Thus, these reactions occur in the normal Marcus regime. For our calculations, the reorganization energy was not needed. We estimated the perturbation of molecular orbital energy at the D and A sites ($\Delta\Delta E$) due to the point dipole generated by C=O groups. For the six-peptide bridge in the α -helical structure comparable to the compound used in Galoppini's experiment, $\Delta\Delta E$ was 24.4 kK in a vacuum or 0.082 V in acetonitrile. From this value, the ratio for the electron transfer in the direction of the molecular dipole vs that against the molecular dipole can be calculated using the equation $k(f)/k(r) = \exp(-\Delta\Delta E/2RT)$. Note that if the reaction is activationless, directional dependence will be very small and hard to detect.

(76) *The Merck Index*, 11th ed; Merck & Co.: Rahway, NJ, 1989; p 63.

(77) Beratan, D. N.; Onuchic, J. N.; Hopfield, J. J. *J. Chem. Phys.* **1987**, *86*, 4488-4498.

(78) Beratan, D. N.; Onuchic, J. N.; Winkler, J. R.; Gray, H. B. *Science* **1992**, *258*, 1740-1741.

(79) Skourtis, S. S.; Beratan, D. N. *J. Biol. Inorg. Chem.* **1997**, *2*, 378-386.

(80) Wuttke, D. S.; Bjerrum, M. J.; Winkler, J. R.; Gray, H. B. *Science* **1992**, *256*, 1007-1009.

(81) Gray, H. B.; Winkler, J. R. *Pure Appl. Chem.* **1992**, *64*, 1257-1262.

(82) Regan, J. J.; Di Bilio, A. J.; Langen, R.; Skov, L. K.; Winkler, J. R.; Gray, H. B.; Onuchic, J. N. *Chem. Biol.* **1995**, *2*, 489-496.

(83) Skov, L. K.; Pascher, T.; Winkler, J. R.; Gray, H. B. *J. Am. Chem. Soc.* **1998**, *120*, 1102-1103.

(84) Beratan, D. N.; Betts, J. N.; Onuchic, J. N. *Science* **1991**, *252*, 1285-1288.

(69) Vassilian, A.; Wishart, J. F.; van Hemelryck, B.; Schwarz, H. A.; Isied, S. *J. Am. Chem. Soc.* **1990**, *112*, 7278-7286.

(70) Isied, S. S.; Vassilian, A.; Wishart, J. *J. Am. Chem. Soc.* **1988**, *110*, 635-637.

(71) Petrov, E. G.; Shevchenko, Y. V.; Teslenko, V. I. *J. Chem. Phys.* **2001**, *115*, 7107-7122.

(72) Okada, A.; Chernyak, V.; Mukamel, S. *J. Phys. Chem.* **1998**, *102*, 1241-1251.

(73) Piotrowiak, P. *Chem. Soc. Rev.* **1999**, *28*, 143-150.

(74) Marcus, R. A.; Sutin, N. *Biochim. Biophys. Acta* **1985**, 265-322.

secondary structures and their conformational dependence on dihedral angles form the basis of the differences in the electronic coupling. The use of π -type donor/acceptor orbitals is more sensitive to the π -interactions between peptide groups. Such studies are models for the interactions of peptide orbitals with low-spin d^5 and d^6 metal complexes. The results presented here can therefore be used to rationalize differences in CT across different peptide secondary structures and in designing ET reactions to take advantage of different peptide conformations as well as direction of ET relative the peptide dipoles.

Conclusions

In this contribution, we used bridging peptides between donors and acceptors to analyze the effects of CT transition energies and the electronic coupling matrix element on the rate of ET. The CT transition energy is dependent on both peptide dipole direction and the ET direction between the donor and acceptor. The electronic coupling for different peptide secondary structures calculated from these energies is dependent on the dihedral angles ϕ and ψ between neighboring peptide residues. Using a cationic dipeptide (representing hole transfer) the charge-shift reaction is found to be significantly more sensitive to changes in dihedral angles than in a similar anionic dipeptide (representing electron transfer). The polyproline II structure, compared to other extended peptide secondary structures (such as the β -strand) is unique as it provides pathways for extended interactions between neighboring peptides. This becomes more important at longer distances, giving an overall smaller decrease in electronic coupling with distance than the other peptide

secondary structures. A stronger interaction in the α -helical secondary structure is less important because of the compactness of the α -helical structure. For example, the five-residue through-space distance for an α -helix is 9.6 Å compared to 16.4 Å in the polyproline II-helix and 19.0 Å for the β -strand structure (Figure 7).

These models are used to account for experimental ET rates across peptides especially in the oligoproline transition metal complexes ($n = 0-3$) where the ET mechanisms are the superexchange type. The effect of peptide dipole on the directional ET rates in α -helices, and proline peptides can also be accounted for using the above analysis. Finally the determination of peptide-peptide electronic coupling (H_{BB}) for peptide radical cations and anions may be useful for placing limits on the interaction between adjacent peptides in different secondary structures.

Acknowledgment. This work was supported by the U.S. Department of Energy, Division of Chemical Science, Office of Basic Energy Sciences under Contracts DE-FG05-90ER 1410 and DE-FG02-93ER 14356. We thank Dr. Norman Sutin and Professor Robert Cave for their helpful comments and Dr. James Wishart for providing the oligoproline coordinates.

Supporting Information Available: Additional data (PDF). This material is available free of charge via the Internet at <http://pubs.acs.org>.

JA020358Q